Acknowledgment. Financial support from the Ministry of Education, Japanese Government (Grant-in-aid 57550543) is acknowledged.

Supplementary Material Available: Spectroscopic data (NMR and IR) of new compounds described in this paper (3 pages). Ordering information is given on any current masthead page.

First Experimental Demonstration of NMR Dynamic Frequency Shifts: Dispersion vs. Absorption (DISPA) Line Shape Analysis of Sodium-23 in Aqueous Sodium Laurate/Lauric Acid Solution

Alan G. Marshall,*† Tao-Chin Lin Wang,†
Charles E. Cottrell,† and Lawrence G. Werbelow‡

Departments of Chemistry and Biochemistry
The Ohio State University, Columbus, Ohio 43210
and Department of Chemistry
New Mexico Tech, Socorro, New Mexico 87801

Received June 21, 1982

One of the most fundamental operating axioms of experimental NMR is that nuclei with the same chemical environment must have the same Larmor frequency (i.e., same chemical shift). However, quadrupolar nuclei of spin >1 (e.g., ^{7}Li, ^{11}B, ^{17}O, ^{23}Na, ^{25}Mg, ^{27}Al, ^{35}Cl, ^{39}K, ^{43}Ca, ^{81}Br, etc.) exhibit two or more types of transitions. For rapid molecular rotational diffusion ($\omega_0\tau_c \ll 1$, where ω_0 is the Larmor frequency and τ_c is the rotational correlation time) all the transitions have the same chemical shift and (exponential) T_1 and T_2 relaxation. For slower motion ($\omega_0\tau_c \gtrsim 1$, as in micelles, membrane vesicles, polymers, or biological macromolecules) the widths and frequencies of the various transitions can be different.[1-4]

For a spin $^3/_2$ nucleus, analysis of the *theoretical* spectrum in Figure 1 clearly shows the two component transitions of different position and width, for $\omega_0\tau_c = 1.2$. For spin $^3/_2$, the relative areas of the two peaks will be 3:2 for any choice of τ_c. Unfortunately, *experimental* demonstration of such a case is not straightforward. First, although the presence of two line widths can be shown,[5-7] the asymmetry in the composite peak is in practice difficult to distinguish from a small phase misadjustment and thus will likely be overlooked. Second, the usual 180°–τ–90° inversion–recovery pulse sequence will not distinguish between the two transitions, because a 90° sampling pulse serves to mix the two longitudinal recovery rates.[4]

The extraordinary sensitivity of the dispersion vs. absorption (DISPA) plot to slight deviations from Lorentzian line shape[8] affords a simple and reliable way to visualize the chemical shift difference between the two peaks. Phase misadjustment acts simply to rotate the DISPA plot[8] and is thus readily distinguished from other non-Lorentzian line shape effects.

Figure 2a shows a ^{23}Na NMR spectrum of ordinary 1.0 M NaCl in D_2O. Although no apodization was applied to the free induction decay from which the absorption and dispersion spectra were computed, the circularity of the accompanying DISPA plot indicates a near-perfect Lorentzian shape for the peak. Thus, any deviations from the DISPA reference circle for other samples will reflect properties of the line shape, rather than any experimental artifacts or signal or data processing.

Figure 2b shows the ^{23}Na NMR spectrum (center) and cor-

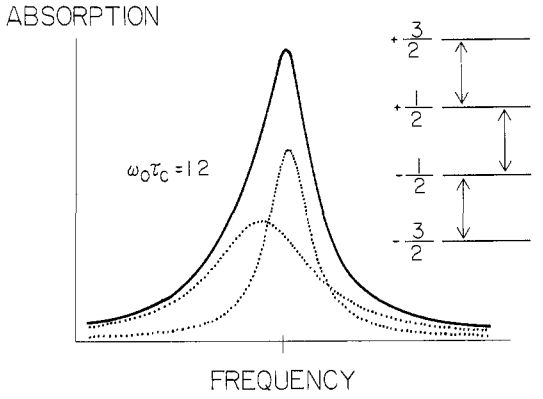

Figure 1. Energy-level diagram (right) and single-quantum NMR spectrum (left) for a spin $^3/_2$ nucleus with rotational correlation time $\tau_c = 1.2/\omega_0 \simeq 15$ ns for ^{23}Na at 7.0 T. The narrow component line arises from the $^{-1}/_2$ to $^{+1}/_2$ transition, and the broad component from the $^{+1}/_2$ to $^{+3}/_2$ and $^{-3}/_2$ to $^{-1}/_2$ transitions. Note the distinct chemical shift difference between the broad and narrow transitions.

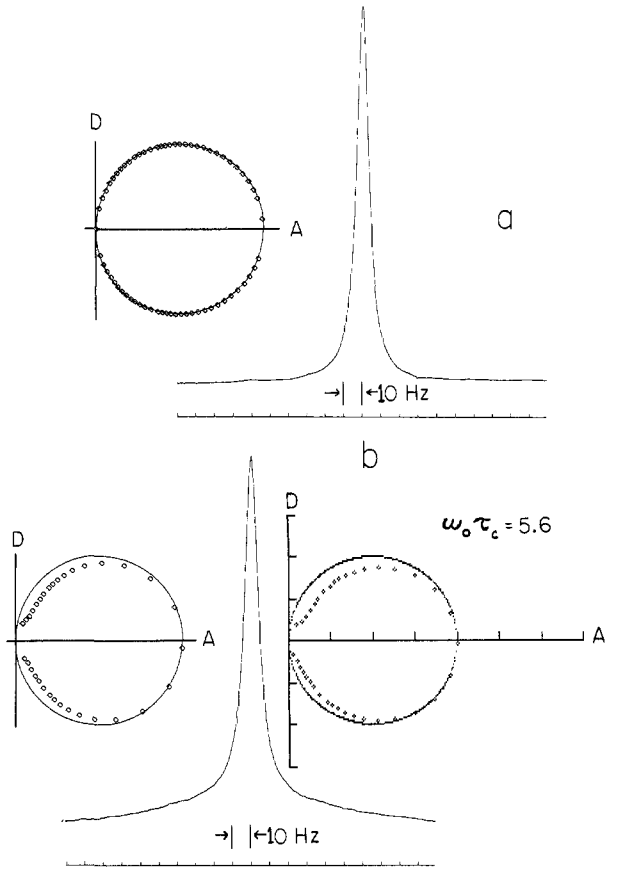

Figure 2. (a) Experimental ^{23}Na NMR spectrum and its corresponding DISPA plot for 1.0 M NaCl in D_2O, obtained from Fourier transformation of an unapodized 4096-point time-domain data set at a spectrometer frequency of 79.388 MHz, with a 90° excitation pulse (44 μs), for one cycle of an 8-pulse phase-alternating sequence. The close fit of the experimental data to the DISPA reference circle indicates a near-perfect Lorentzian line shape. (b) Experimental ^{23}Na NMR spectrum and its corresponding DISPA plot (left) for 120 mM NaCl, 20 mM sodium laurate, and 5 mM lauric acid in aqueous (15% D_2O) solution. The sample was milky white, with a sodium laurate concentration of about twice the critical micelle concentration for 0.1 M NaCl solutions of sodium laurate.[13] Detection was as in Figure 2a, except for 20° excitation pulse width. The experimental DISPA plot (left) closely matches that computed for $\omega_0\tau_c = 5.6$ (right), as discussed in the text.

† The Ohio State University.
‡ New Mexico Tech.

(1) Hubbard, P. S. *J. Chem. Phys.* **1970**, *53*, 985–987.
(2) Werbelow, L. G. *J. Chem. Phys.* **1979**, *70*, 5381–5383.
(3) Fouques, C. E. M.; Werbelow, L. G. *Can. J. Chem.* **1979**, *57*, 2329–2332.
(4) Werbelow, L. G.; Marshall, A. G. *J. Magn. Reson.* **1981**, *43*, 443–448.
(5) Monoi, J.; Uedaira, H. *J. Magn. Reson.* **1980**, *38*, 119–129.
(6) Shporer, M.; Civan, M. M. *Biophys. J.* **1972**, *12*, 114–122.
(7) Laszlo, P. *Angew. Chem., Int. Ed. Engl.* **1978**, *17*, 254–266.
(8) Marshall, A. G. In "Fourier, Hadamard, and Hilbert Transforms in Chemistry"; Marshall, A. G., Ed.; Plenum Press: New York, 1982; pp 99–123.

0002-7863/82/1504-7665$01.25/0

responding experimental DISPA plot (left) for sodium ion in a laurate/lauric acid sample. The spectrum was phased by minimizing rotation of the DISPA plot.[8] A series of theoretical DISPA plots were then constructed for various choices of τ_c. The DISPA curve at lower right in Figure 2b gave the closest theoretical match to the experimental case and corresponds to $\omega_0\tau_c = 5.6$, for which the two component peak widths have a ratio of 13.71:1.

It is of course conceivable that the frequency difference demonstrated in Figure 2 could be due to two *chemically* different ^{23}Na environments, each represented by a single Lorentzian line. Three facts argue very strongly against that interpretation. First, a least-squares fit of the absorption signal of Figure 2b, in which the two peak positions, widths, and intensities were allowed to vary *independently*, gave two peaks of relative area 1.46:1 $\simeq$ 1.5:1, and relative widths of 13.72:1 (both exactly the same as from the DISPA simulation). It is highly improbable that two different chemical environments would happen to have relative populations (3:2) exactly the same as for the two components of a dynamic frequency-shifted pair of lines. Second, a 180°-τ-10° inversion-recovery experiment (not shown) clearly resolved the longitudinal relaxation of the broad and narrow component peaks, with a T_1 difference consistent with the line width and frequency shift differences predicted by the DISPA simulation. Finally, the close match between the experimental DISPA data and the DISPA curve simulated for a dynamic frequency-shifted system further supports the present interpretation.

In conclusion, dynamic frequency shifts have been predicted[9,10] and observed[11,12] in ESR and predicted in NMR.[1-4] The present paper provides the first convincing expermental demonstration of multiple peak positions and widths for quadrupolar nuclei in NMR. A useful result of the present analysis is that the rotational correlation time, τ_c, can be determined from a *single* experimental spectrum. It is suggested that future NMR studies using quadrupolar nuclei to probe chemical and motional environment at slowly tumbling sites (e.g., micelles, membrane vesicles, polymers, biological macromolecules) should employ DISPA analysis to detect any dynamic frequency shifts and use them to determine rotational correlation times. Full details of the data reduction[14] and theoretical simulations for DISPA analysis of NMR spectra of spin $^3/_2$ nuclei will be published elsewhere.

Acknowledgment. This work was supported by the donors of the Petroleum Research Fund, administered by the American Chemical Society.

Registry No. Na, 7440-23-5; sodium laurate, 629-25-4; lauric acid, 143-07-7.

(9) Fraenkel, G. F. *J. Chem. Phys.* **1965**, *42*, 4275-4298.
(10) Baram, A.; Luz, Z.; Alexander, S. *J. Chem. Phys.* **1973**, *58*, 4558-4564.
(11) Poupko, R.; Baram, A.; Luz, Z. *Mol. Phys.* **1974**, *27*, 1345-1357.
(12) Poupko, R.; Luz, Z. *Mol. Phys.* **1978**, *36*, 733-752.
(13) Mukerjee, P.; Mysels, K. J. *Natl. Stand. Ref. Data Ser.* (*U.S., Natl. Bur. Stand.*) **1971**, 138.
(14) Wang, T.-C. L.; Cottrell, C. E.; Marshall, A. G. *Comput. Chem.*, in press.

Silicon-Induced Fragmentations: Stereoselective Preparation of (*Z*,*E*)- and (*Z*,*Z*)-1,4-Dienamine Derivatives. Synthesis of (9*Z*,12*E*)-Tetradecadien-1-yl Acetate, Pheromone of Various Lepidoptera[1]

N. V. Bac and Y. Langlois*

Institut de Chimie des Substances Naturelles du CNRS 91190 Gif-sur-Yvette, France

Received August 4, 1982

During the past decade, the synthesis of pheromones of Lepidoptera, which are generally found as straight chain mono- or polyolefinic acetates, alcohols, or aldehydes, attracted increasing attention.[2,3] Highly stereoselective methods were developed for the synthesis of these chemical messengers which are often active as a mixture of components in accurate proportions. Our approach to the synthesis of conjugated dienes using 2-alkylpyridines as starting material gave access to various *Z*,*E*, *E*,*E*,[4] and *E*,*Z*[5] pheromones.

Scheme I

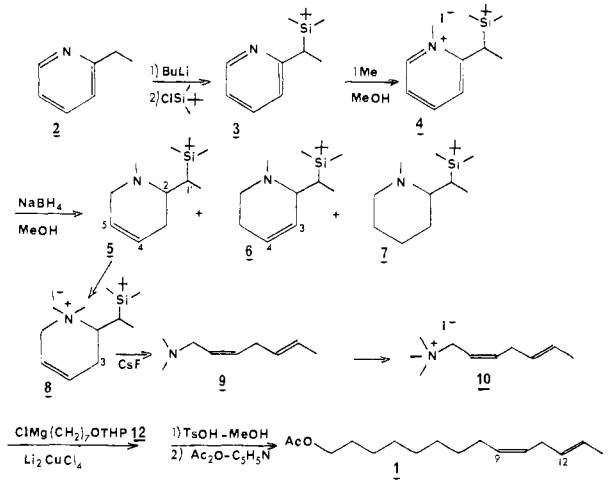

Scheme II

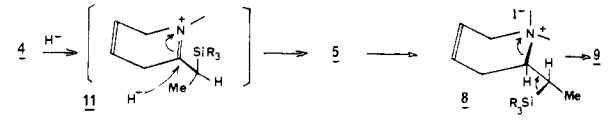

We report herein a new methodology leading to (*Z*,*E*)- and (*Z*,*Z*)-1,4-dienamine derivatives **9** and **15** by a fluoride ion induced silicon fragmentation or by a "sila-Cope" elimination. The dienamine **9** is a direct synthetic precursor of the (9*Z*,12*E*)-tetradecadien-1-yl acetate (**1**) pheromone of various Lepidoptera.[6]

Thus the carbanion of 2-ethylpyridine formed with *n*-butyllithium (1.1 equiv) in tetrahydrofuran at −70 °C reacts readily with tert-butyldimethylchlorosilane (1.1 equiv, −70 to 0 °C) and led to the pyridine derivative **3** (83%). This compound after treatment with an excess of methyl iodide gave rise to the corresponding pyridinium salt **4**, which when reduced with sodium borohydride in methanol, afforded products **5**–**7** in 76%, 8%, and 5% yield, respectively. The spectral characteristics and in particular 400-MHz ^{1}H NMR decoupling experiments were consistent with the proposed structure for those compounds.

Alkylation of the 1,2,3,6-tetrahydropyridine **5** with methyl

(1) Preliminary disclosure: First French-Japanese Symposium on Medicinal and Fine Chemistry, Lake Biwa, Moriyama City, Japan, May 1981.

(2) Henrick, C. A. *Tetrahedron* **1977**, *33*, 1845.
(3) Rossi, R. *Synthesis* **1977**, 817.
(4) Decodts, G.; Dressaire, G.; Langlois, Y. *Synthesis* **1979**, 510.
(5) Dressaire, G.; Langlois, Y. *Tetrahedron Lett.* **1980**, *21*, 67.
(6) Henrick, C. A. *Tetrahedron* **1977**, *33*, 1867 and references therein.
(7) NMR (400 MHz, Me_4Si = 0 ppm, $CDCl_3$) δ (**5**) 0.03 and 0.10 (3 H × 2, 2 s, CH_3Si), 0.89 (9 H, s, *t*-BuSi), 1.08 (3 H, d, $J_{2'-1'}$ = 7 Hz, $C_{2'}H_3$), 1.18 (1 H, m, C_1H), 2.03 (2 H, m, C_3H_2), 2.29 (3 H, s, NCH_3), 2.62 (1 H, m, C_2H), 3.09 and 3.21 (2 H, dd, $J_{HH'}$ = 18 Hz, C_6-H and C_6-H'), 5.63 (1 H, d, J_{4-5} = 10 Hz, C_5H), 5.75 (1 H, d, J_{4-5} = 10 Hz, C_4H); (**6**) −0.04 and 0.08 (3 H × 2, 2 s, CH_3Si), 0.92 (9 H, s, *t*-BuSi), 1.07 (3 H, d, $J_{2'-1'}$ = 7 Hz, $C_{2'}H_3$), 1.45 (1 H, m, C_1H), 1.93 and 1.98 (2 H, 2 m, C_5H and C_5H'), 2.33 (3 H, s, NCH_3), 2.60 (1 H, m, C_2H), 2.83 (2 H, m, C_6H_2), 5.65 (1 H, br d, J_{3-4} = 10 Hz, C_3H), 5.73 (1 H, m, C_4H); (**10**) 1.65 (3 H, d, J_{7-6} = 6.3 Hz, C_7H_3), 3.05 (2 H, t, C_4H_2), 3.45 (6 H, s, $N(CH_3)_2$), 4.36 (2 H, d, J_{1-2} = 8.5 Hz, C_1H_2), 5.40 and 5.44 (1 H, 2 t, J_{5-6} = 15.2 Hz, J_{4-5} = 6.3 Hz, C_5H), 5.61 (1 H, m, C_6H), 5.64 and 5.67 (1 H, 2t, J_{2-3} = 11 Hz, J_{1-2} = 8.5 Hz, C_2-H), 6.20 and 6.22 (1 H, 2 t, J_{2-3} = 11 Hz, J_{3-4} = 7.6 Hz, C_3H); (**1**) 1.30 (12 H, m, C_2–C_7), 1.60 and 1.65 (m and d, J_{13-14} = 6 Hz, C_8H_2 and $C_{14}H_3$), 2.05 (3 H, s, $OCOCH_3$), 2.73 (2 H, m, $C_{11}H_2$), 4.07 (2 H, t, J_{1-2} = 7 Hz, C_1H_2), 5.34–5.51 (4 H, 2 m, C_9H, $C_{10}H$, $C_{12}H$, and $C_{13}H$); (**16**, $CDCl_3$ + CF_3CO_2H) 1.15 (9 H, s, *t*-BuSi), 1.6 (3 H, dd, J_{7-6} = 7 Hz, J_{7-5} = 1.6 Hz, C_7H_3), 2.8 (2 H, m, C_4H_2), 3.06 (3 H, s, NCH_3), 4.06 (2 H, m, C_1H_2), 5.21 (1 H, m, J_{5-6} = 10.5 Hz, J_{4-5} = 7 Hz, J_{7-5} = 1.6 Hz, C_5H), 5.53 (2 H, m, C_2H and C_6H), 6.05 (1 H, 2 t, J_{2-3} = 11 Hz, J_{3-4} = 7 Hz, C_3-H), 7.5–8 (10 H, m, ArH).

0002-7863/82/1504-7666$01.25/0